

## Finite-temperature ordering in two-dimensional magnets

Alessandro Cuccoli, Tommaso Roscilde, Valerio Tognetti, and Paola Verrucchi

*Dipartimento di Fisica dell'Università di Firenze and Istituto Nazionale di Fisica della Materia (INFN), Largo E. Fermi 2, I-50125 Firenze, Italy*

Ruggero Vaia

*Istituto di Elettronica Quantistica del Consiglio Nazionale delle Ricerche, via Panciatichi 56/30, I-50127 Firenze, Italy and Istituto Nazionale di Fisica della Materia (INFN), Largo E. Fermi 2, I-50125 Firenze, Italy*

(Received 13 March 2000)

We study the two-dimensional quantum Heisenberg antiferromagnet on the square lattice with easy-axis exchange anisotropy. By the semiclassical method called pure-quantum self-consistent harmonic approximation we analyze several thermodynamic quantities and investigate the existence of a finite temperature transition, possibly describing the low-temperature critical behavior experimentally observed in many layered real compounds. We find that an Ising-like transition characterizes the model even when the anisotropy is of the order of  $10^{-2}J$  ( $J$  being the intralayer exchange integral), as in most experimental situations. On the other hand, typical features of the isotropic Heisenberg model are observed for both values of anisotropy considered, one in the *quasi*-isotropic limit and the other in a more markedly easy-axis region. The good agreement found between our theoretical results and the experimental data relative to the real compound  $\text{Rb}_2\text{MnF}_4$  shows that the insertion of the easy-axis exchange anisotropy, with quantum effects properly taken into account, provides a quantitative description and explanation of the experimental data, thus allowing us to recognize in such anisotropy the main agent for the observed onset of finite temperature long-range order.

### I. INTRODUCTION

In recent years the increasing interest in the physics of low-dimensional magnets has led to a deep analysis of the thermodynamic behavior of two-dimensional quantum antiferromagnets<sup>1</sup> and, in particular, of the isotropic quantum Heisenberg antiferromagnet on the square lattice (QHAF).<sup>2,3</sup> Such a model has in fact been widely used to describe the magnetic properties of many quasi-two-dimensional real compounds, from the  $S=1/2$  cuprate  $\text{La}_2\text{CuO}_4$ <sup>4,5</sup> to the  $S=5/2$  compound  $\text{Rb}_2\text{MnF}_4$ , recently studied by Lee *et al.*<sup>6</sup>

Different theoretical methods<sup>7-12</sup> have been used to examine the rich reservoir of experimental data and the picture of the subject is now well focused, albeit with some shaded parts. In particular open questions still exist<sup>13-16</sup> on the low-temperature region, where the spin correlation length becomes of the order of  $10^2$  lattice spacings and the real magnets are seen to develop macroscopic areas of correlated spins.

The theoretical debate on the low-temperature regime has been mainly dedicated to the isotropic QHAF, but real compounds are not actually well described by such an isotropic model when temperature is lowered: the experimental evidence of a finite-temperature transition, opposite to the Mermin-Wagner theorem<sup>17</sup> assertion that such a transition cannot occur in the two-dimensional isotropic QHAF, suggests that three-dimensional correlations and possible anisotropy effects, as well as a combination of both, must be considered.

The magnetic structure of layered real compounds is such that the exchange integral  $J$  for neighboring spins belonging to the same plane is orders of magnitude larger than that for neighboring spins on different planes,<sup>18-20</sup> hereafter called

$J'$ ; one would hence naively expect the magnetic properties to be those of an effective two-dimensional magnet down to temperatures of the order of  $J'$ , until the transition towards an ordered three-dimensional phase should take place. However, the experimentally observed transition occurs at a critical temperature of the order of  $J$ , signaling the transition itself to be driven by the intralayer exchange interaction; details of such interaction, such as possible easy-axis or easy-plane anisotropies, are hence fundamental in the analysis of the critical behavior.

Several works (see Ref. 21 for a review) have shown that, besides the superexchange interaction, there exist further interaction mechanisms whose effects may be taken into account by inserting proper anisotropy terms in the magnetic Hamiltonian; in particular, the transition observed in  $\text{K}_2\text{NiF}_4$  ( $S=1$ ),<sup>20</sup>  $\text{Rb}_2\text{FeF}_4$  ( $S=2$ ),<sup>20</sup>  $\text{K}_2\text{MnF}_4$ ,<sup>22</sup>  $\text{Rb}_2\text{MnF}_4$  ( $S=5/2$ ),<sup>20</sup> and others, is seen to be possibly due to an easy-axis anisotropy. Such anisotropy has often been described in the literature via an external staggered magnetic field: This choice, despite allowing a qualitative description of the experimental data, lacks the fundamental property of describing a genuine phase transition, as the field explicitly breaks the symmetry and makes the model ordered at all temperatures.

In order to produce a second order transition known to be due to an easy-axis anisotropy, it is actually appropriate to insert such anisotropy in the form of an exchange one, thus preserving the symmetry under inversion along the easy axis, whose spontaneous breaking manifests itself in the transition: The subject of this paper is the study of the thermodynamic properties of the resulting model, hereafter called easy-axis QHAF (EA-QHAF).

In Sec. II we define the model and discuss its general

properties, posing the problems we want to address. The method used is briefly described in Sec. III, where results for several thermodynamic quantities and different values of the anisotropy are shown and commented on. In Sec. IV we compare our results with the available experimental data for the staggered magnetization and susceptibility, and for the correlation length, of the  $S=5/2$  real compound  $\text{Rb}_2\text{MnF}_4$ ,<sup>6,20</sup> while conclusions are drawn in Sec. V.

## II. MODEL AND METHOD

The EA-QHAF on the square lattice is described by the Hamiltonian

$$\hat{\mathcal{H}} = \frac{J}{2} \sum_{\mathbf{i}, \mathbf{d}} [\mu (\hat{S}_{\mathbf{i}}^x \hat{S}_{\mathbf{i}+\mathbf{d}}^x + \hat{S}_{\mathbf{i}}^y \hat{S}_{\mathbf{i}+\mathbf{d}}^y) + \hat{S}_{\mathbf{i}}^z \hat{S}_{\mathbf{i}+\mathbf{d}}^z], \quad (1)$$

where  $\mathbf{i}=(i_1, i_2)$  runs over the sites of a square lattice,  $\mathbf{d}$  connects each site to its four nearest neighbors,  $J>0$  is the antiferromagnetic exchange integral, and  $\mu$  is the anisotropy parameter ( $0 \leq \mu < 1$  for easy-axis models). The spin operators  $\hat{S}_{\mathbf{i}}^\alpha$  ( $\alpha=x, y, z$ ) are such that  $|\hat{\mathbf{S}}|^2 = S(S+1)$  and obey  $[\hat{S}_{\mathbf{i}}^\alpha, \hat{S}_{\mathbf{j}}^\beta] = i \varepsilon_{\alpha\beta\gamma} \delta_{\mathbf{i}\mathbf{j}} \hat{S}_{\mathbf{i}}^\gamma$ .

When  $\mu=1$  the model loses its easy-axis character and reduces to the isotropic QHAF. The  $\mu=0$  case will be hereafter called *Ising limit*, not to be confused with the genuine *Ising model*,<sup>23</sup> reproduced by Eq. (1) with  $\mu=0$  and  $S=1/2$ . Despite being a very particular case of Eq. (1), the two-dimensional Ising model on the square lattice is a fundamental point of reference for the study of the thermodynamic properties of the EA-QHAF.

In particular, a renormalization-group analysis of the classical counterpart of the model Eq. (1)<sup>24,25</sup> foresees the occurrence of an Ising-like transition at finite temperature for any value of  $\mu$ , no matter how near to the isotropic value  $\mu=1$ ; this analysis is supported by several works based on classical Monte Carlo simulations.<sup>26-29</sup>

In the quantum case, however, no information is given about the value of the critical temperature  $T_c(\mu, S)$  as a function of anisotropy and spin, save the fact that  $T_c(0, 1/2) = 0.567J$  and  $T_c(1, S) = 0$ . Hence we do not know whether or not the small anisotropy ( $|\mu-1| \approx 10^{-2}$ ) observed in real compounds can be responsible of transitions occurring at critical temperatures of the order on  $J$ , given also the fact that we expect quantum fluctuations to lower the critical temperature with respect to the classical case.

We have developed a quantitative analysis of several thermodynamic properties of the model, by means of the semi-classical method called pure-quantum self-consistent harmonic approximation (PQSCHA),<sup>30-32</sup> already successfully applied to many magnetic systems in one and two dimensions. The method reduces quantum expressions for statistical averages to effective classical-like ones, containing temperature and spin-dependent renormalization parameters. The thermodynamics of the effective model can then be studied by means of classical techniques, like Monte Carlo simulations.

The PQSCHA is known to be particularly suitable for anisotropic (easy-plane or easy-axis) models, but it also gives very good results in the isotropic QHAF so that we can confidently use it to investigate the possible crossover be-

tween a Heisenberg-like behavior at high temperature and an Ising-like one near  $T_c$ ; such crossover is detected in the experimental data to such an extent that, well above the transition, real compounds can be satisfactorily described by the isotropic QHAF.

## III. RESULTS

The main output of the PQSCHA is the effective Hamiltonian appearing in all statistical averages, whose expression for the model described by Eq. (1) reads

$$\mathcal{H}_{\text{eff}} = -\frac{1}{2} J \bar{S}^2 \sum_{\mathbf{i}, \mathbf{d}} [\theta_{\perp}^4 \mu (s_{\mathbf{i}}^x s_{\mathbf{i}+\mathbf{d}}^x + s_{\mathbf{i}}^y s_{\mathbf{i}+\mathbf{d}}^y) + \theta_{\parallel}^2 \theta_{\perp}^2 s_{\mathbf{i}}^z s_{\mathbf{i}+\mathbf{d}}^z] + \mathcal{G}(t, \bar{S}), \quad (2)$$

where  $\mathbf{s}=(s^x, s^y, s^z)$  is a classical unit vector,  $\bar{S}=S+1/2$ , and  $t=T/J\bar{S}^2$  is the reduced temperature hereafter used. The appearance of the minus sign in front of the effective Hamiltonian is due to the fact that in Eq. (2), as in all the classical-like expressions reported below, spins belonging to one of the two sublattices have been flipped, to simplify the notation and because this is an innocuous operation at a classical level.

The renormalization parameters are

$$\theta_{\parallel}^2 = 1 - \frac{\mathcal{D}_{\parallel}}{2}, \quad \theta_{\perp}^2 = 1 - \frac{\mathcal{D}_{\perp}}{2}, \quad (3)$$

where the coefficients

$$\begin{aligned} \mathcal{D}_{\parallel} &= \frac{1}{N\bar{S}} \sum_{\mathbf{k}} \frac{a_{\mathbf{k}}}{b_{\mathbf{k}}} (1 - \mu \gamma_{\mathbf{k}}) \mathcal{L}_{\mathbf{k}}, \\ \mathcal{D}_{\perp} &= \frac{1}{N\bar{S}} \sum_{\mathbf{k}} \frac{a_{\mathbf{k}}}{b_{\mathbf{k}}} \left(1 - \frac{\gamma_{\mathbf{k}}}{\mu}\right) \mathcal{L}_{\mathbf{k}} \end{aligned} \quad (4)$$

are self-consistently determined by solving Eqs. (3) and (4) with

$$a_{\mathbf{k}}^2 = 4(\theta_{\parallel}^2 + \mu \theta_{\perp}^2 \gamma_{\mathbf{k}}), \quad b_{\mathbf{k}}^2 = 4(\theta_{\parallel}^2 - \mu \theta_{\perp}^2 \gamma_{\mathbf{k}}), \quad (5)$$

and

$$\gamma_{\mathbf{k}} = \frac{1}{4} \sum_{\mathbf{d}} e^{i\mathbf{k} \cdot \mathbf{d}}, \quad \mathcal{L}_{\mathbf{k}} = \coth f_{\mathbf{k}} - \frac{1}{f_{\mathbf{k}}}, \quad f_{\mathbf{k}} = \frac{a_{\mathbf{k}} b_{\mathbf{k}}}{2\bar{S}t},$$

$\mathbf{k}$  being the wave vector in the first Brillouin zone.

The temperature and spin-dependent uniform term

$$\mathcal{G}(t, \bar{S}) = 2J\bar{S}^2(1 - \theta_{\parallel}^2 \theta_{\perp}^2) + J\bar{S}^2 t \sum_{\mathbf{k}} \ln \left( \frac{\sinh f_{\mathbf{k}}}{\theta_{\perp}^2 f_{\mathbf{k}}} \right),$$

does not enter the expressions for the statistical averages, but contributes to the free energy and to the related thermodynamic quantities.

The renormalization coefficients  $\mathcal{D}_{\parallel}$  and  $\mathcal{D}_{\perp}$  measure the pure-quantum fluctuations parallel and perpendicular to the easy axis, respectively, of one spin with respect to its nearest neighbors, and vanish in both the high-temperature and the classical  $S \rightarrow \infty$  limit. It is worthwhile noticing that the fluc-

tuations along the easy-axis only enters the renormalization of the  $z$ -component of the exchange interaction.

Defining the effective exchange integral and effective anisotropy

$$J_{\text{eff}} = J \theta_{\parallel}^2 \theta_{\perp}^2, \quad \mu_{\text{eff}} = \mu \frac{\theta_{\perp}^2}{\theta_{\parallel}^2}$$

Eq. (2) can be written in the form

$$\mathcal{H}_{\text{eff}} = -\frac{1}{2} J_{\text{eff}} \bar{S}^2 \sum_{\mathbf{i}, \mathbf{d}} [\mu_{\text{eff}} (s_{\mathbf{i}}^x s_{\mathbf{i}+\mathbf{d}}^x + s_{\mathbf{i}}^y s_{\mathbf{i}+\mathbf{d}}^y) + s_{\mathbf{i}}^z s_{\mathbf{i}+\mathbf{d}}^z] + \mathcal{G}(t, \bar{S}), \quad (6)$$

to make evident that the PQSCHA leads to a classical-like effective model of the same form as the original quantum one, whose thermodynamic properties can be studied by classical numerical technique, properly taking into account the spin and temperature dependence of the renormalized parameters  $J_{\text{eff}}$  and  $\mu_{\text{eff}}$ . As  $\theta_{\parallel}^2 < \theta_{\perp}^2 < 1$ , it is  $J_{\text{eff}} < J$  and  $1 > \mu_{\text{eff}} > \mu$ , so that quantum effects are seen to cause the weakening of both the exchange interaction and the easy-axis anisotropy; in the isotropic limit  $\mathcal{D}_{\parallel} = \mathcal{D}_{\perp}$  and  $\mu_{\text{eff}} = \mu = 1$ .

The PQSCHA expression for the statistical average of a quantum operator  $\hat{O}$  is

$$\langle \hat{O} \rangle = \frac{1}{\mathcal{Z}_{\text{eff}}} \int d^N \mathbf{s} O_{\text{eff}} e^{-\beta \mathcal{H}_{\text{eff}}}, \quad (7)$$

where  $\beta = T^{-1}$ ,  $\mathcal{Z}_{\text{eff}} = \int d^N \mathbf{s} e^{-\beta \mathcal{H}_{\text{eff}}}$ ;  $O_{\text{eff}}$  is determined by the same procedure leading to  $\mathcal{H}_{\text{eff}}$  and contains temperature and spin dependent renormalizations; after Eq. (7) most thermodynamic quantities may be written in a particularly suggestive form in terms of classical-like statistical averages defined by the effective Hamiltonian

$$\langle \dots \rangle_{\text{eff}} = \frac{1}{\mathcal{Z}_{\text{eff}}} \int d^N \mathbf{s} (\dots) e^{-\beta \mathcal{H}_{\text{eff}}};$$

as far as the evaluation of  $\langle \dots \rangle_{\text{eff}}$  is concerned, one must keep in mind that, because of the temperature dependence of the effective anisotropy appearing in  $\mathcal{H}_{\text{eff}}$ , each point in temperature corresponds to a different effective model. This means that if the classical Monte Carlo technique is used, as done in this work, the simulated model changes with temperature so that, at variance with the isotropic case, no existing classical data can be used and a complete series of *ad hoc* simulations must be carried on. Nevertheless, the computational effort required is still that of a classical simulation, as the evaluation of the renormalized parameters is a matter of a few seconds on a standard PC.

The application of the PQSCHA to the EA-QHAF leads to the following results for the thermodynamic quantities we have considered:

(i) *Internal energy*  $u \equiv \langle \hat{\mathcal{H}} \rangle / (NJ\bar{S}^2)$ :

$$u = \frac{1}{NJ\bar{S}^2} \langle \mathcal{H}_{\text{eff}} \rangle_{\text{eff}} - \mathcal{G}(t, \bar{S}) + \mathcal{F}(t, \bar{S}), \quad (8)$$

where

$$\mathcal{F} = -2(\theta_{\perp}^2 - \theta_{\parallel}^2) \left[ \theta_{\perp}^2 + \frac{2}{1 - \mu^2} (\theta_{\perp}^2 - \theta_{\parallel}^2) \right]$$

is a negative zero-point quantum correction term due to the anisotropy (it vanishes in the isotropic limit).

(ii) *Staggered magnetization*  $m \equiv \Sigma_{\mathbf{i}} (-1)^{i_1+i_2} \langle \hat{S}_{\mathbf{i}}^z \rangle / N\bar{S}$ :

$$m = \theta_{\perp}^2 \langle s_{\mathbf{i}}^z \rangle_{\text{eff}} + \mathcal{M}(t, S); \quad (9)$$

where the magnetization renormalization is seen to be due to an effective spin reduction ( $\theta_{\perp}^2 < 1$ ) and to the appearance of the negative term  $\mathcal{M} = -(\theta_{\perp}^2 - \theta_{\parallel}^2)/(1 - \mu^2)$  which vanishes in the isotropic limit and is finite for  $\mu = 0$ .

(iii) *Staggered correlation function* above  $T_c$

$G(r) \equiv (-1)^{r_1+r_2} \langle \hat{\mathbf{S}}_{\mathbf{i}} \cdot \hat{\mathbf{S}}_{\mathbf{i}+\mathbf{r}} \rangle / \bar{S}^2$  with  $\mathbf{r} = (r_1, r_2)$  any vector of the square lattice and  $r = |\mathbf{r}|$ :

$$G(r) = \theta_{\mathbf{r}}^4 \langle \mathbf{s}_{\mathbf{i}} \cdot \mathbf{s}_{\mathbf{i}+\mathbf{r}} \rangle_{\text{eff}}, \quad (10)$$

where  $\theta_{\mathbf{r}}^2 = 1 - \mathcal{D}_{\mathbf{r}}/2$  and

$$\mathcal{D}_{\mathbf{r}} = \frac{1}{N\bar{S}} \sum_{\mathbf{k}} \frac{a_{\mathbf{k}}}{b_{\mathbf{k}}} (1 - \cos(\mathbf{k} \cdot \mathbf{r})) \mathcal{L}_{\mathbf{k}}$$

is a further site-dependent renormalization coefficient. For increasing  $r$ , the coefficient  $\mathcal{D}_{\mathbf{r}}$  rapidly converges to a uniform term, so that the asymptotic ( $r \rightarrow \infty$ ) behavior of  $G(r)$  is actually determined by that of the effective classical-like correlation function  $\langle \mathbf{s}_{\mathbf{i}} \cdot \mathbf{s}_{\mathbf{i}+\mathbf{r}} \rangle_{\text{eff}}$ .

(iv) *Staggered static susceptibility* above  $T_c$

$\chi \equiv \Sigma_{\mathbf{r}} G(r)/3$ :

$$\chi = \frac{1}{3} \left[ \frac{S(S+1)}{\bar{S}^2} + \sum_{\mathbf{r} \neq 0} G(r) \right]. \quad (11)$$

(v) *Correlation length* above  $T_c$ .

We have determined the correlation length  $\xi$  by fitting  $G(r)$  with the expression proposed by Serena, Garcia, and Levanyuk<sup>28</sup>

$$G(r) \propto \frac{1}{\xi^{1/4}} \frac{e^{-r/\xi}}{(r/\xi)^{1/2} + (r/\xi)^{1/4}}, \quad (12)$$

which interpolates the two asymptotic behaviors  $r \rightarrow \infty$  and  $r \rightarrow 0$  of the Ising model.<sup>33</sup>

In what follows, we show our results as obtained combining the above PQSCHA expressions with the numerical output of the classical Monte Carlo simulations we have performed to evaluate the effective statistical averages  $\langle \dots \rangle_{\text{eff}}$ . At variance with the isotropic case, where results for different values of the spin are obtained by the same series of classical simulations, we now have to fix the value of the spin in order to determine, for a given value of  $\mu$ , the corresponding  $\mu_{\text{eff}}$  to be used in the simulation. We have hence concentrated on the case  $\mu = 0.9942$  and  $S = 5/2$ , because these are anisotropy and spin values corresponding to the real compound  $\text{Rb}_2\text{MnF}_4$ ; the more anisotropic case  $\mu = 0.7$  and  $S = 5/2$  has also been considered, because of its expectedly more marked Ising-like features.

In Figs. 1 and 2 we show the internal energy and specific heat versus temperature for both values of  $\mu$ , compared with the isotropic case<sup>12</sup>  $\mu = 1$ . As the value of the critical tem-

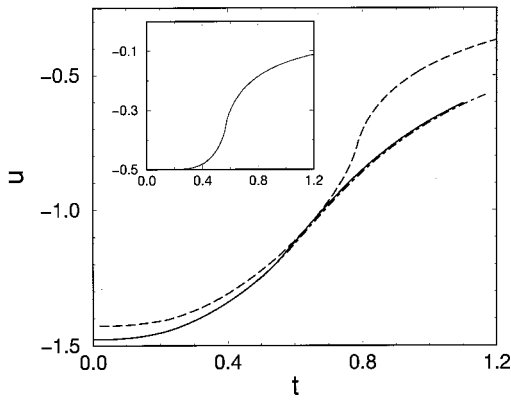


FIG. 1. Internal energy vs  $t$  for  $S=5/2$  and  $\mu=0.7$  (dashed), 0.9942 (full), 1 (dash-dotted); the curve relative to the Ising model ( $S=1/2$  and  $\mu=0$ ) is shown in the inset.

perature increases for larger anisotropy, but diminishes when smaller spin values are considered, we avoid the confusing direct comparison between our curves ( $\mu > 0$ ,  $S=5/2$ ) and the corresponding quantities for the Ising model ( $\mu=0$ ,  $S=1/2$ ), by showing the latter as insets.

The Ising character of the  $\mu=0.7$  model is evidenced by the pronounced peak in the specific heat, corresponding to a qualitatively different temperature dependence of the internal energy with respect to that of the isotropic model. Although such a difference is almost not perceptible when the  $\mu=0.9942$  curve is considered, a clear peak in the specific heat is still present, testifying to a persistence of the Ising-like behavior even in this *quasi*-isotropic model.

The same conclusion is drawn when the staggered magnetization is considered: in Fig. 3 we see that for  $\mu=0.9942$  there exists a wide temperature range where the system is ordered, with a critical temperature  $t_c$  that, despite being lower than the one relative to the  $\mu=0.7$  case, is still of the order of  $J$ . In the inset we show the magnetization curves normalized to their saturation values, as functions of  $t/t_c$ , together with that of the Ising model: It is evident that an increased anisotropy causes a sharpening of the way the magnetization vanishes.

The critical temperatures hereafter used are  $t_c=0.785$  for  $\mu=0.7$  and  $t_c=0.575$  for  $\mu=0.9942$ ; these values have been determined by locating at best the correlation length divergence and consistently coincide with those emerging from

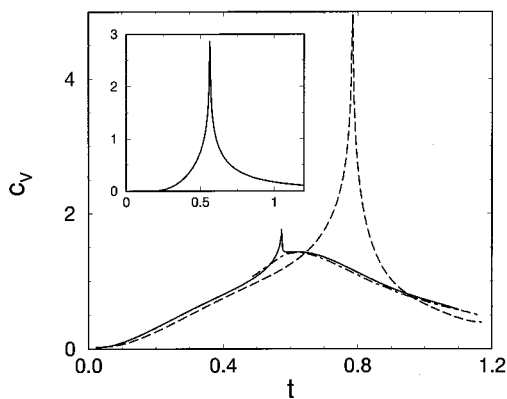


FIG. 2. Specific heat vs  $t$  (lines and inset as in Fig. 1).

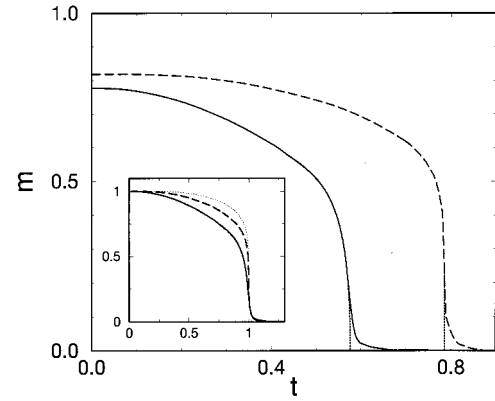


FIG. 3. Staggered magnetization vs  $t$  for  $S=5/2$  and  $\mu=0.7$  (dashed), 0.9942 (full); the dotted lines are the data fits used to extract the critical temperature values. In the inset the same curves, normalized to the saturation value, are shown vs  $t/t_c$ , together with the magnetization of the Ising model (dotted).

the analysis of the critical behavior of other quantities. For instance the critical temperatures determined by fitting the magnetization curves (see the dotted lines in Fig. 3) are  $t'_c=0.787$  for  $\mu=0.7$  and  $t'_c=0.576$  for  $\mu=0.9942$ .

It should be noted that even below  $t_c$ , where the finite value of the magnetization would suggest a complete predominance of the Ising character, the system does actually display features which are distinctive of the isotropic model. In particular, the specific heat for both values of  $\mu$  shows, after an exponential start typical of a gapped dispersion relation, a change in the curvature and a temperature dependence of the same type of that characterizing the isotropic model. It is just in the vicinity of  $t_c$  that a new change in the curvature announces the forthcoming transition.

In Fig. 4 we show the correlation function  $G(r)$  as a function of  $r$  in the quasi-isotropic case  $\mu=0.9942$  and for three different temperatures. The fit of our data with the Serena–Garcia–Levanyuk function, Eq. (12), is very good in the whole temperature range examined, and hence leads to a clean evaluation of the correlation length.

In Fig. 5 we show the correlation length and also report the curve for the isotropic model:<sup>12</sup> we notice that the  $\mu=0.9942$  curve lays on the isotropic one up to correlation

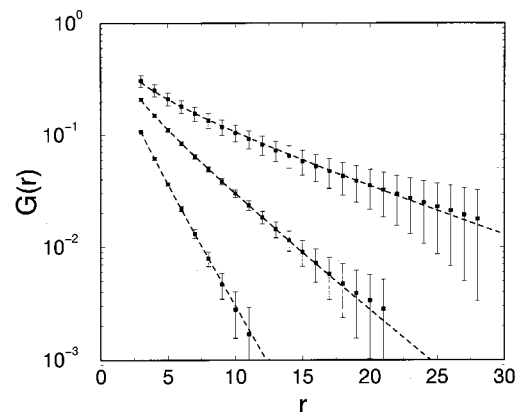


FIG. 4. Correlation functions for  $S=5/2$ ,  $\mu=0.9942$ , and  $t=0.6, 0.7, 0.85$  (from the top); dotted lines are fits with the Serena–Garcia–Levanyuk function (see text).

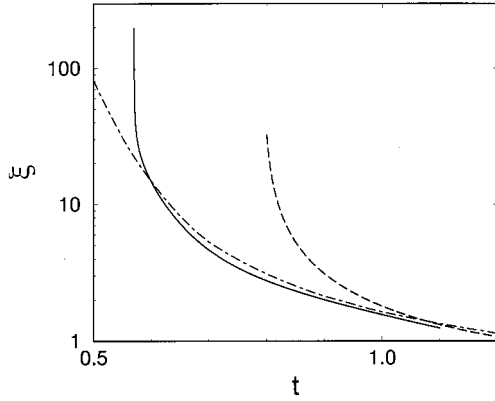


FIG. 5. Correlation length vs  $t$  for  $S=5/2$  and  $\mu=0.7$  (dashed), 0.9942 (full), 1 (dash-dotted).

lengths of the order of 20 lattice spacings (i.e.,  $t \approx 1.03t_c$ ), while for  $\mu=0.7$  a deviation is evident already for  $\xi \approx 2$  (i.e.,  $t \approx 1.3t_c$ ). This means that, in the former case, there is a temperature region where the model significantly behaves like the isotropic model, as far as the correlation length is concerned, and it is hence meaningful to introduce the idea of a crossover from a Heisenberg- to an Ising-like regime;<sup>6</sup> on the contrary, when  $\mu=0.7$  the Ising character of the model is manifest already when correlations over a few lattice spacings develop.

#### IV. COMPARISON WITH EXPERIMENTAL DATA

The results shown in Sec. III qualitatively explain the mechanism possibly underlying the finite-temperature ordering experimentally observed in many *quasi*-two dimensional real magnets.

As for a more precise quantitative analysis, we have concentrated ourselves on the  $S=5/2$  magnet  $\text{Rb}_2\text{MnF}_4$ : The reason for this choice is the availability of recent neutron scattering data<sup>6</sup> relative to such compound and the fact that, because of its crystallographic structure,  $\text{Rb}_2\text{MnF}_4$  is known to behave as a two-dimensional magnet both above and below the observed transition.<sup>20,34</sup> This means that the critical behavior is not contaminated by the onset of three-dimensional order and a clean characterization of the transition is possible, as well as a meaningful comparison with the experimental data for the magnetization below  $T_c$ .

The model parameters  $J_s = 7.62 \pm 0.09$  K and  $\mu_s = 0.9953$  available in the literature<sup>35</sup> for the compound  $\text{Rb}_2\text{MnF}_4$  are obtained by fitting the extrapolated  $T \rightarrow 0$  experimental data for the spin-wave frequencies with the expression

$$\omega_{\mathbf{k}} = 4J_s S \sqrt{\frac{1}{\mu_s^2} - \gamma_{\mathbf{k}}^2}; \quad (13)$$

this means that  $J_s$  and  $\mu_s$  are renormalized by the zero-point quantum fluctuations and are not the bare values to be inserted in Eq. (1). These have hence been determined equating Eq. (13) with the zero-temperature dispersion relation relative to the EA-QHAF as given by the PQSCHA

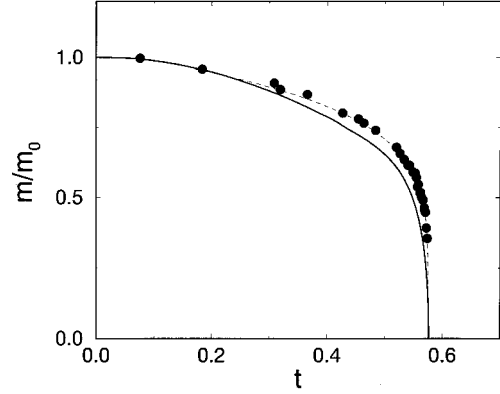


FIG. 6. Staggered magnetization vs  $t$  for  $\text{Rb}_2\text{MnF}_4$ , normalized to the saturation value  $m_0$ : our results (full line) are compared with experimental data (full circles) from Ref. 20; the dashed line is the interpolating curve therein proposed.

$$\omega_{\mathbf{k}} = 4J\tilde{S}\mu\theta_{\perp}^2(0) \sqrt{\frac{\theta_{\parallel}^4(0)}{\mu^2\theta_{\perp}^4(0)} - \gamma_{\mathbf{k}}^2}, \quad (14)$$

where  $\theta_{\parallel}^2(0)$  and  $\theta_{\perp}^2(0)$  are the renormalization parameters defined in Eq. (3) evaluated at  $t=0$ .

The resulting equation for  $\mu$

$$\mu = \mu_s \frac{\theta_{\parallel}^2(0)}{\theta_{\perp}^2(0)}$$

must be self-consistently solved, as both  $\theta_{\perp}$  and  $\theta_{\parallel}$  depend on  $\mu$ , and gives  $\mu=0.9942$ .

Once  $\mu$  is determined, the equation for the exchange integral

$$J = \frac{S}{\tilde{S}} \frac{J_s}{\mu\theta_{\perp}^2(0)}$$

is straightforwardly solved and gives  $J=7.42$  K.

In Fig. 6 our results for the staggered magnetization are shown together with the experimental data from Ref. 20 and the interpolating curve there proposed. Besides the overall agreement in the whole ordered phase, it should be noted that

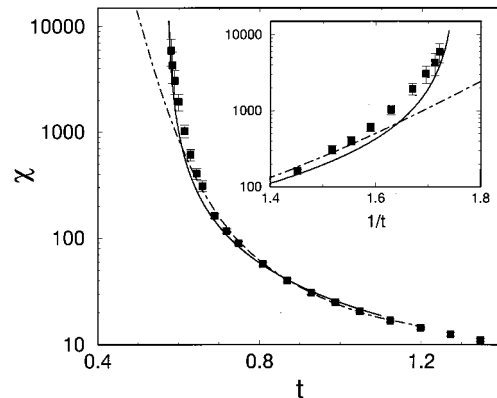


FIG. 7. Staggered susceptibility vs  $t$  for  $S=5/2$ ,  $\mu=0.9942$  (full), and  $\mu=1$  (dashed-dotted); symbols are neutron scattering data on  $\text{Rb}_2\text{MnF}_4$  from Ref. 6. A zoom of the critical region is shown in the inset.

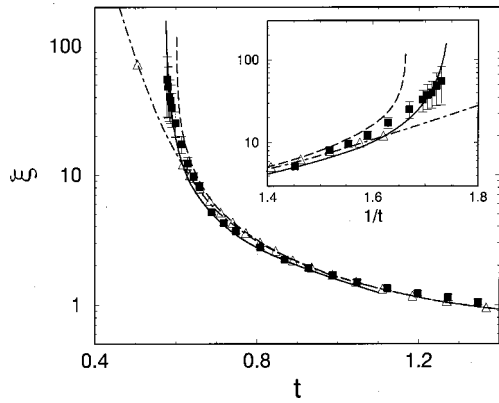


FIG. 8. Correlation length vs  $t$ ; lines, symbols, and inset as in Fig. 7 apart from the dashed curve, representing the result of a mean-field approach to the anisotropy proposed in Ref. 6, and the triangles, which are quantum Monte Carlo data for the isotropic model, from Ref. 16.

our prediction for the value of the critical temperature perfectly coincides with the one deriving from the experimental analysis, which gives  $T_c = 38.4$  K (i.e.,  $t_c = 0.575$ ); such a large value of  $T_c$  with respect to the exchange integral  $J = 7.42$  K should not surprise us, as the squared value of the spin has been actually extracted from the latter.

In order to obtain the best quantitative description of the EA-QHAF in the paramagnetic phase, and given the small anisotropy of  $\text{Rb}_2\text{MnF}_4$ , the lowest-temperature data for the staggered susceptibility and correlation length, shown in Figs. 7 and 8, are determined by the PQSCHA version introduced in Ref. 12 and there shown to be the most appropriate to study the isotropic model. The difference between such a version and the original one described in Sec. II consists in the appearance of the renormalization parameters  $\kappa_{\parallel,\perp}^2$ , instead of  $\theta_{\parallel,\perp}^2$ , in Eqs. (5), with  $\kappa_{\parallel,\perp}^2 = \theta_{\parallel,\perp}^2 - \mathcal{D}_{\parallel,\perp}^{\text{cl}}/2$ ,  $\mathcal{D}_{\parallel,\perp}^{\text{cl}}$  being the renormalization coefficients determined by the classical self-consistent harmonic approximation.

The agreement between our results and the experimental data is indeed noticeable, given also the fact that no best-fit procedure has been used. In addition, our results represent a clear improvement with respect to those coming from a mean-field treatment of the anisotropy, as proposed by Keimer *et al.*,<sup>5</sup> which enables one to derive the correlation length of the anisotropic model directly from the data of the isotropic one, as done in Ref. 6 starting from the PQSCHA results for the isotropic model<sup>12</sup> itself. In particular, it is evident from Fig. 8 that the mean-field approach, apart from accounting for the existence of the phase transition, leads to an overestimate of the critical temperature, while the model with exchange anisotropy gives a very accurate estimate of  $t_c$ .

## V. CONCLUSIONS

In this work we have studied the easy-axis quantum Heisenberg antiferromagnet on the square lattice by means of the pure-quantum self-consistent harmonic approximation; expressions for several quantum statistical averages have been determined for the general model, with any value of the spin and of the anisotropy. The numerical work, consisting of classical Monte Carlo simulations on a properly renormalized model, have been concentrated on the  $S = 5/2$ ,  $\mu = 0.7$  and  $S = 5/2$ ,  $\mu = 0.9942$  cases, the latter corresponding to the real compound  $\text{Rb}_2\text{MnF}_4$ .

We have shown that a finite temperature transition is present in both cases and that such a transition is clearly of an Ising type; the value of the corresponding critical temperature has been determined by the analysis of the correlation length dependence on temperature and has been always found to perfectly agree with that extracted by the analysis of other thermodynamic quantities.

Despite the essential presence of the transition, the EA-QHAF also display (both below and above  $t_c$ ) features which are typical of the isotropic model. In the ordered phase it is the specific heat behavior that testifies to the existence of isotropic-like excitations. On the other hand, when the critical region is abandoned in the paramagnetic phase, the anisotropy loses its fundamental role and a crossover towards the isotropic behavior is observed, at least as far as the correlation length is concerned; such crossover, however, has a weaker meaning for larger anisotropy, being confined already for  $\mu = 0.7$  to the high-temperature region where  $\xi$  is the order of the lattice spacing and differences between different models become irrelevant.

We have compared our theoretical results with the neutron scattering experimental data for the staggered magnetization, staggered susceptibility, and correlation length of the real compound  $\text{Rb}_2\text{MnF}_4$  and found an excellent agreement both for the overall temperature behavior and for the value of the critical temperature.

We can hence conclude that the experimentally observed finite temperature transition in  $\text{Rb}_2\text{MnF}_4$  is due to an easy-axis anisotropy in the intralayer exchange interaction and that, despite the small value of the anisotropy, the compound shows an Ising-like critical behavior.

## ACKNOWLEDGMENTS

We acknowledge Professor R. J. Birgeneau and Dr. Y. S. Lee for sending us preprints and experimental data. This work has been partially supported by the COFIN98-MURST fund.

<sup>1</sup>For a relatively early review, see *Magnetic Properties of Layered Transition Metal Compounds*, edited by L.J. de Jongh (Kluwer, Dordrecht, 1990).

<sup>2</sup>E. Manousakis, *Rev. Mod. Phys.* **63**, 1 (1991).

<sup>3</sup>M.A. Kastner, R.J. Birgeneau, G. Shirane, and Y. Endoh, *Rev.*

*Mod. Phys.* **70**, 897 (1998).

<sup>4</sup>G. Shirane, Y. Endoh, R.J. Birgeneau, M.A. Kastner, Y. Hidaka, M. Oda, M. Suzuki, and T. Murakami, *Phys. Rev. Lett.* **59**, 1613 (1987).

<sup>5</sup>B. Keimer, N. Belk, R.J. Birgeneau, A. Cassanho, C.Y. Chen, M.

- Greven, M.A. Kastner, A. Aharony, Y. Endoh, R.W. Erwin, and G. Shirane, *Phys. Rev. B* **46**, 14 034 (1992).
- <sup>6</sup>Y.S. Lee, M. Greven, B.O. Wells, R.J. Birgeneau, and G. Shirane, *Eur. Phys. J. B* **5**, 15 (1998).
- <sup>7</sup>D.P. Arovas and A. Auerbach, *Phys. Rev. B* **38**, 316 (1988).
- <sup>8</sup>M. Takahashi, *Phys. Rev. B* **40**, 2494 (1989).
- <sup>9</sup>S. Chakravarty, B.I. Halperin, and D.R. Nelson, *Phys. Rev. B* **39**, 2344 (1989).
- <sup>10</sup>P. Hasenfratz and F. Niedermayer, *Phys. Lett. B* **268**, 231 (1991).
- <sup>11</sup>N. Elstner, A. Sokol, R.R.P. Singh, M. Greven, and R.J. Birgeneau, *Phys. Rev. Lett.* **75**, 938 (1995); N. Elstner, *Int. J. Mod. Phys. B* **11**, 1753 (1997).
- <sup>12</sup>A. Cuccoli, V. Tognetti, R. Vaia, and P. Verrucchi, *Phys. Rev. Lett.* **77**, 3439 (1996); *Phys. Rev. B* **56**, 14 456 (1997).
- <sup>13</sup>B.B. Beard, R.J. Birgeneau, M. Greven, and U.-J. Wiese, *Phys. Rev. Lett.* **80**, 1742 (1998).
- <sup>14</sup>J.K. Kim and M. Troyer, *Phys. Rev. Lett.* **80**, 2705 (1998).
- <sup>15</sup>P. Hasenfratz, *Eur. Phys. J. B* **13**, 11 (2000).
- <sup>16</sup>B. B. Beard, V. Chudnovsky, and P. Keller-Marxer, cond-mat/9910291 (unpublished).
- <sup>17</sup>N.D. Mermin and H. Wagner, *Phys. Rev. Lett.* **17**, 1133 (1966).
- <sup>18</sup>M.E. Lines, *Phys. Rev.* **164**, 736 (1967).
- <sup>19</sup>R.J. Birgeneau, H.J. Guggenheim, and G. Shirane, *Phys. Rev. Lett.* **22**, 720 (1969).
- <sup>20</sup>R.J. Birgeneau, H.J. Guggenheim, and G. Shirane, *Phys. Rev. B* **1**, 2211 (1970).
- <sup>21</sup>J. Kanamori, in *Magnetism*, Vol. 1, edited by G.T. Rado and H. Suhl (Academic, New York, 1963).
- <sup>22</sup>R.J. Birgeneau, H.J. Guggenheim, and G. Shirane, *Phys. Rev. B* **8**, 304 (1973).
- <sup>23</sup>L. Onsager, *Phys. Rev.* **65**, 117 (1944).
- <sup>24</sup>M. Bander and D.L. Mills, *Phys. Rev. B* **38**, 12 015 (1988).
- <sup>25</sup>T. Roscilde, Tesi di Laurea, University of Florence, 1999.
- <sup>26</sup>J.D. Patterson and G.L. Jones, *Phys. Rev. B* **3**, 131 (1971).
- <sup>27</sup>K. Binder and L.P. Landau, *Phys. Rev. B* **13**, 1140 (1976).
- <sup>28</sup>P.A. Serena, N. García, and A. Levanyuk, *Phys. Rev. B* **47**, 5027 (1993).
- <sup>29</sup>M.E. Gouvêa, G.M. Wysin, S.A. Leonel, A.S.T. Pires, T. Kampeter, and F.G. Mertens, *Phys. Rev. B* **59**, 6229 (1999).
- <sup>30</sup>A. Cuccoli, V. Tognetti, P. Verrucchi, and R. Vaia, *Phys. Rev. A* **45**, 8418 (1992).
- <sup>31</sup>A. Cuccoli, R. Giachetti, V. Tognetti, R. Vaia, and P. Verrucchi, *J. Phys.: Condens. Matter* **7**, 7891 (1995).
- <sup>32</sup>A. Cuccoli, V. Tognetti, R. Giachetti, R. Maciocco, and R. Vaia, *Physica A* **271**, 387 (1999).
- <sup>33</sup>L.P. Kadanoff, W. Götze, D. Hamblen, R. Hecht, E.A.S. Lewis, V.V. Palciauskas, M. Rayl, and J. Swift, *Rev. Mod. Phys.* **39**, 395 (1967).
- <sup>34</sup>R.A. Cowley, G. Shirane, R.J. Birgeneau, and H.J. Guggenheim, *Phys. Rev. B* **15**, 4292 (1977).
- <sup>35</sup>H.W. de Wijn, L.R. Walker, and R.E. Walstedt, *Phys. Rev. B* **8**, 285 (1973).